JETIR.ORG ISSN: 2349-5162 | ESTD Year : 2014 | Monthly Issue
JOURNAL OF EMERGING TECHNOLOGIES AND INNOVATIVE RESEARCH (JETIR)
An International Scholarly Open Access, Peer-reviewed, Refereed Journal

A mathematical investigation of SIR model of Covid-19 populations considering all three infectious stages

[1] ***Satyendra Singh Yadav,*** [2] ***Anurag Paliwal,***

[1]Professor, [2]Research Scholar
[1-2] *Narain (P.G.) College, Shikohabad, Dist.-Firozabad*
Affiliated at Dr. Bhimrao Ambedkar University Agra, U.P. (India)

Abstract: In this article, we go over a mathematical SIR model that takes into account all five states of the COVID-19 population. To create the model, we segmented the population into five categories based on their health: susceptible, mild, moderate, and severe infected, and recovered. We have determined where the suggested model's disease-free and endemic equilibrium points are located. The basic reproduction number, model stability, and the existence and uniqueness of solutions have all been derived. Graphical representations of numerical results have also been developed for sensitivity analysis. The model's dynamical behavior was analyzed in great detail. Analytical and numerical demonstrations of the disease-free equilibrium point, the endemic equilibrium point, and the fundamental reproduction number were presented in this model. Local asymptotic stability was observed for the disease-free equilibrium point if $R_0 < 1$, but not if $R_0 > 1$. This finding suggests that people's efforts to safeguard themselves can have a major impact on the prevalence of the disease in the community at large. Notably, assessing the possibility for sustained transmission to occur in new locations requires an understanding of the dynamics of infection spread and an evaluation of the efficiency of control efforts. The model can be used to explain the spread of epidemics in different parts of the world.

Keywords-Basic Reproduction number, Stability, Covid-19, Equilibrium points

I. INTRODUCTION

The spread of the Corona virus has become a major threat in today's globe. As of May 6, 2020, there have been approximately 3588777 confirmed cases of COVID-19, including 247503 deaths. Lockdown, social isolation, and masks are currently being used by nearly the entire global population to combat this pandemic. Similarly, India is employing such measures as present to combat the pandemic. The SARS-CoV-2 family includes the COVID-19 pandemic. There is currently no treatment available for this illness. COVD-2019 is an epidemic that spreads rapidly from person to person through the air or through direct contact with an infected person. Therefore, COVID-2019 is an infectious illness. This illness has a short 2-14 day incubation period. A recent study suggested a 2% to 3% global fatality rate due to the COVID-19 pandemic. For those above the age of 60, this condition is fatal. People over the age of 40 face an overall 27% death rate. A COVID-19 patient was discovered in India on January 20, 2020. This individual travelled all the way from Wuhan, China to Kerala, India. At the end of November 2019, in the Chinese city of Wuhan, the first case of COVID-19 was discovered. Following January 30, 2020, the corona virus gradually spread across India.

Since the first reported instances of coronavirus disease-19 (COVID-19) in India, scientists from a variety of disciplines have tried to mathematically simulate the spread of the virus. At first glance, it is clear that existing models differ greatly in terms of their purview, assumptions, predictions, timeliness, accuracy, impact on health care services, and so on. As a result, we conducted a brief review to synthesize narratives and evaluate the agreement between expected and actual case outcomes in India.

Alanazi et al. (2020) suggested developing a model for predicting COVID-19 by utilising the SIR and machine learning in order to improve both the quality of health care provided in the Kingdom of Saudi Arabia (KSA) and the general well-being of its

population. The model determined whether COVID-19 will circulate throughout the population or become extinct over the course of time. Cooper et al. (2020) investigated the efficacy of the modelling technique on the pandemic caused by the spreading of the novel COVID-19 disease and developed a susceptible-infected-removed (SIR) model that offers a theoretical framework to explore the disease's propagation within a community. This model was used to study the effectiveness of the modelling approach. Kotwal et al. (2020) carried out research in the form of a rapid assessment of the mathematical models utilised for the prediction of Coronavirus illness (COVID-19) in India for the purpose of narrative synthesis and to evaluate the correlation between the predicted and actual value of cases in India. A new model of coronavirus-19 illness (COVID-19) was developed by Akyildiz and Alshammari (2021). This new model is a complex fractional SIR epidemic model with a nonstandard nonlinear incidence rate and a recovery, where the derivative operator has a Mittag-Leffler kernel in the Caputo sense (ABC). During the time period that was examined, Franco and Dutra (2021) noticed that the effective reproduction number in the state of Paraba followed a pattern that was decreasing. Lakshmi and Sabarmathi (2021) explored how numerical simulations can be used to provide light on the potential for COVID-19 in the Tirupathur district of Tamilnadu, India, to illustrate the flow of variables associated with the model. In addition to this, they investigated the analysis of recovered for both allopathy and Siddha treatments. Malavika et al. (2021) utilized the Logistic growth curve model for short-term prediction. They used SIR models to estimate the maximum number of active cases and peak time. Finally, they used the Time Interrupted Regression model to analyze the impact of lockdown and other interventions. A modified age-structured SIR model was provided by Ram and Schaposnik (2021). This model was based on known patterns of social interaction and distance measurements within the state of Washington, which is located in the United States. They came to the conclusion that the age distribution of a population has a major impact on the rate at which a disease spreads and the number of deaths it causes, as well as on the effectiveness of age-specific contact and treatment methods. Mohajan (2022) demonstrated that COVID-19 is lethal over time and made a prediction regarding whether or not the disease will continue to spread or go extinct entirely. His research places an emphasis on the importance of vaccination in lowering the risk of contracting the disease. It is able to determine the minimum number of individuals who should be vaccinated in order to achieve herd immunity against COVID-19. The distribution pattern and dynamics of the Covid-19 dissemination were studied by Saxena et al. (2023), who used the SIR model as their foundation. They were able to generate an analytical estimation for the virus' span of existence, its longevity, growing pattern, and other characteristics by using the dynamics of the model.

II. THE DEVELOPMENT OF A MATHEMATICAL MODEL

In this work, the dynamics and effects of Covid-19 on the human population are studied using a five-dimensional deterministic model. The current model divides the world's population into five distinct groups. Here are some details about each category:

(i) Susceptible individuals: This segment of the human population is generally free of disease, however they are vulnerable to contracting Covid-19. $S(t)$stands for the potential patient pool size at a given time.

(ii) Mild infectious individuals: This group of people has a low prevalence of Covid-19 infection. $I_1(t)$is the average size of Covid-19 individuals at time t. If these patients receive prompt and appropriate care, they have a recovery rate ofγ_1.

(iii) Moderate infectious individuals: These people have a moderate case of Covid-19 infection. $I_2(t)$. is the population size of Covid-19 at time t. These people can either recover at a rate of $\gamma_2 < \gamma_1$ or pass away from the illness.

(iv) Severe infectious individuals: Individuals belonging to this group have a severe case of Covid-19 infection. Covid-19 population size at time t is represented by $I_3(t)$. These people have a chance of being cured at a rate of $\gamma_3 < \gamma_2 < \gamma_1$, or they could die from their illness.

(v) Recovered individuals: Those who are able to overcome any form of infection. $R(t)$ represents the population size after recovery.

Table-1: Transitions between the compartments of COVID-19 models

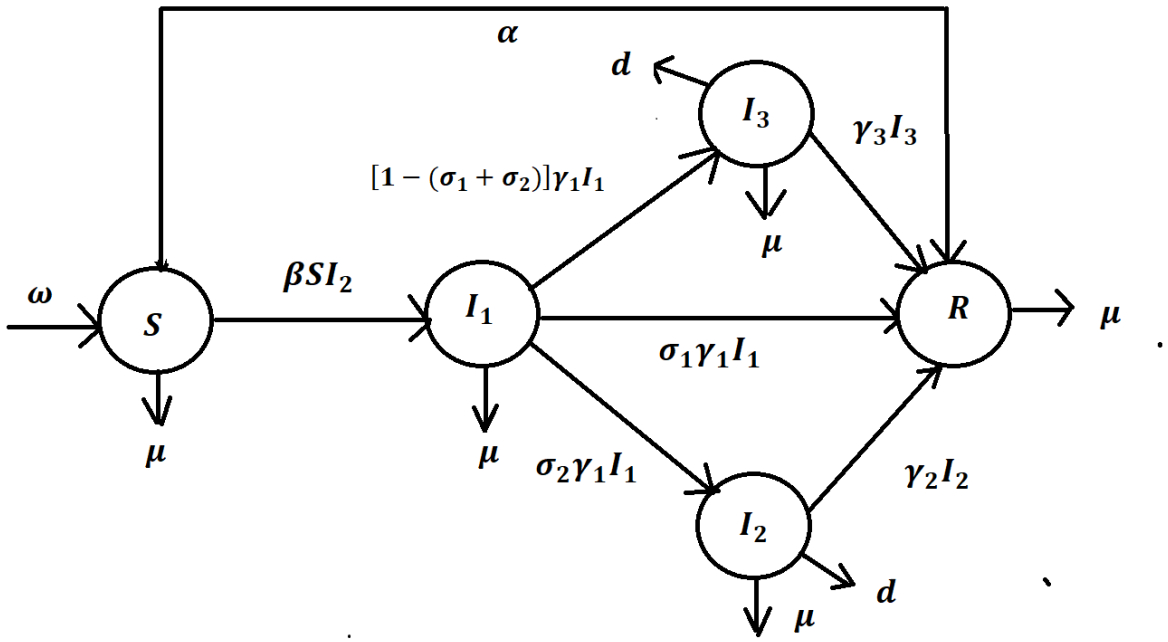

Five ordinary differential equations (ODEs) are shown below to represent the aforementioned Covid-19 phase transition.

$$\frac{dS}{dt} = \omega - \alpha S - \mu S - \beta S I_2 \quad (1)$$

$$\frac{dI_1}{dt} = \beta S I_2 - \sigma_1\gamma_1 I_1 - \sigma_2\gamma_1 I_1 - [1-(\sigma_1+\sigma_2)]\gamma_1 I_1 - \mu I_1 \quad (2)$$

$$\frac{dI_2}{dt} = \sigma_2\gamma_1 I_1 - \gamma_2 I_2 - \mu I_2 - d I_2 \quad (3)$$

$$\frac{dI_3}{dt} = [1-(\sigma_1+\sigma_2)]\gamma_1 I_1 - \gamma_3 I_3 - \mu I_3 - d I_3 \quad (4)$$

$$\frac{dR}{dt} = \sigma_1\gamma_1 I_1 + \gamma_2 I_2 + \gamma_3 I_3 + \alpha S - \mu R \quad (5)$$

Where $N = S + I_1 + I_2 + I_3 + R$

Table-1: Definitions and ranges for various parameters

Parameters	Meaning	Values
ω	Human susceptibility to compartment $S(t)$ recruitment rate	0.045
μ	Humanity's innately low survival rate	0.6
β	Transition infectious rate	0.5
σ_1	Fraction who suffers with moderate COVID-19	0.07
σ_2	Fraction who suffers with severe COVID-19	0.1
γ_1	Recovery rate from mild infection by natural immunity	0.7
γ_2	Recovery rate from moderate infection by natural immunity	0.5
γ_3	Recovery rate from severe infection by natural immunity	0.2
d	Moderate and severe disease induced death rate	0.5
α	Recovery rate of susceptible humans	0.1

III. INVARIANT REGION

In this scenario, we'll assume the entire population is

$$N(t) = S + I_1 + I_2 + I_3 + R \quad (7)$$

By doing a time derivative on both sides of (7), we obtain

$$\frac{dN}{dt} = \frac{dS}{dt} + \frac{dI_1}{dt} + \frac{dI_2}{dt} + \frac{dI_3}{dt} + \frac{dR}{dt} \quad (8)$$

Equation (8) is obtained by plugging in equations (1-5)

$N'(t) = \omega - \mu N - d I_1 - d I_2 \leq \Lambda - \mu N$

$N'(t) \leq \omega - \mu N$ (9)

Differential equation (9) is solved for $N(t)$, and we obtain

$N(t) \leq \left(\frac{\omega}{\mu}\right) - \left[\frac{\omega}{\mu} - N(0)\right] e^{-\mu t}$ (10)

Now as $t \longrightarrow \infty$,Reducing equation (10) to its simplest form,

$N(t) \leq \frac{\omega}{\mu}$ (11)

we have, $0 \leq N(t) \leq \frac{\omega}{\mu}$

As a result, there exist bounds on all human population solution variables.

$\Omega = \left\{(S, I_1, I_2, I_3, R) \in R_+^5 : 0 \leq N(t) \leq \frac{\omega}{\mu}\right\}$. (12)

IV. EQUILIBRIUM POINTS ANALYSIS

(i) Disease free equilibrium (DFE): In (1-5), the equilibrium point when the SIR model is disease-free is shown to be

$I_1 = I_2 = I_3 = R = 0$

Thus $\omega - \alpha S - \mu S = 0$

$S = \frac{\omega}{\alpha+\mu}$

$E_0\left(\frac{\omega}{\alpha+\mu}, 0,0,0,0,0,0,0,0\right)$is the disease free equilibrium points.

(ii)Endemic equilibrium points: When an epidemic continues to ravage a neighbourhood, the model (1-5) reaches its endemic equilibrium point E^*. We used a steady-state evaluation of the system (1-5) to derive the following result:

$\omega - \alpha S - \mu S - \beta S I_2 = 0$ (13)

$\beta S I_2 - \sigma_1 \gamma_1 I_1 - \sigma_2 \gamma_1 I_1 - [1 - (\sigma_1 + \sigma_2)]\gamma_1 I_1 - \mu I_1 = 0$ (14)

$\sigma_2 \gamma_1 I_1 - \gamma_2 I_2 - \mu I_2 - d I_2 = 0$ (15)

$[1 - (\sigma_1 + \sigma_2)]\gamma_1 I_1 - \gamma_3 I_3 - \mu I_3 - d I_3 = 0$ (16)

$\gamma_1 I_1 + \gamma_2 I_2 + \gamma_3 I_3 + \alpha S - \mu R = 0$ (17)

$\omega - \alpha S - \mu S - \beta S I_2 = 0$

$S(\alpha + \mu) + \beta S I_2 = \omega$

$(\alpha + \mu) + \beta I_2 = \frac{\omega}{S}$

$\beta I_2 + (\alpha + \mu) = \frac{\omega}{S}$

$\beta I_2 = \frac{\omega}{S} - (\alpha + \mu)$

$I_2 = \frac{\omega}{\beta S} - \frac{(\alpha+\mu)}{\beta}$

$\beta S I_2 - \sigma_1 \gamma_1 I_1 - \sigma_2 \gamma_1 I_1 - [1 - (\sigma_1 + \sigma_2)]\gamma_1 I_1 - \mu I_1 = 0$

$\beta S I_2 - \gamma_1 I_1 - \mu I_1 = 0$

$\beta S I_2 = (\gamma_1 + \mu) I_1$

$S = \frac{\gamma_1+\mu}{\beta}\frac{I_1}{I_2}$

$S^* = \frac{(\gamma_1+\mu)(\gamma_2+\mu+d)}{\beta\sigma_2\gamma_1}$ (18)

$I_2 = \frac{\omega}{\beta S} - \frac{(\alpha+\mu)}{\beta}$

$I_2 = \frac{\omega}{(\gamma_1+\mu)}\frac{I_2}{I_1} - \frac{(\alpha+\mu)}{\beta}$

$I_2 = \frac{\omega}{(\gamma_1+\mu)}\frac{\sigma_2\gamma_1}{\gamma_2+\mu+d} - \frac{(\alpha+\mu)}{\beta}$

$I_2^* = \frac{\omega\sigma_2\gamma_1}{(\gamma_1+\mu)(\gamma_2+\mu+d)} - \frac{(\alpha+\mu)}{\beta}$ (19)

$$\sigma_2\gamma_1 I_1 - \gamma_2 I_2 - \mu I_2 - dI_2 = 0$$

$$\sigma_2\gamma_1 I_1 = \gamma_2 I_2 + \mu I_2 + dI_2 = (\gamma_2 + \mu + d)I_2$$

$$I_1 = \frac{1}{\sigma_2\gamma_1}(\gamma_2 + \mu + d)I_2$$

$$\frac{I_1}{I_2} = \frac{1}{\sigma_2\gamma_1}(\gamma_2 + \mu + d)$$

$$\frac{I_2}{I_1} = \frac{\sigma_2\gamma_1}{\gamma_2+\mu+d} I_1 = \frac{1}{\sigma_2\gamma_1}(\gamma_2 + \mu + d)\left[\frac{\omega\sigma_2\gamma_1}{(\gamma_1+\mu)(\gamma_2+\mu+d)} - \frac{(\alpha+\mu)}{\beta}\right]$$

$$I_1^* = \frac{\omega}{(\gamma_1+\mu)} - \frac{(\alpha+\mu)(\gamma_2+\mu+d)}{\beta\sigma_2\gamma_1}$$

$$[1-(\sigma_1+\sigma_2)]\gamma_1 I_1 - \gamma_3 I_3 - \mu I_3 - dI_3 = 0 \quad (20)$$

$$I_3 = \frac{[1-(\sigma_1+\sigma_2)]\gamma_1}{\gamma_3+\mu+d} I_1$$

$$I_3 = \frac{[1-(\sigma_1+\sigma_2)]\gamma_1}{\gamma_3+\mu+d}\left[\frac{\omega}{(\gamma_1+\mu)} - \frac{(\alpha+\mu)(\gamma_2+\mu+d)}{\beta\sigma_2\gamma_1}\right]$$

$$I_3^* = \frac{\omega\gamma_1[1-(\sigma_1+\sigma_2)]}{(\gamma_1+\mu)(\gamma_3+\mu+d)} - \frac{(\alpha+\mu)(\gamma_2+\mu+d)[1-(\sigma_1+\sigma_2)]}{\beta\sigma_2(\gamma_3+\mu+d)} \quad (21)$$

$$\sigma_1\gamma_1 I_1 + \gamma_2 I_2 + \gamma_3 I_3 + \alpha S - \mu R = 0$$

$$R = \frac{1}{\mu}(\alpha S + \sigma_1\gamma_1 I_1 + \gamma_2 I_2 + \gamma_3 I_3)$$

$$R^* = \frac{1}{\mu}\left[\frac{(\gamma_1+\mu)(\gamma_2+\mu+d)\alpha}{\beta\sigma_2\gamma_1} + \frac{\omega\sigma_1\gamma_1}{(\gamma_1+\mu)} - \frac{(\alpha+\mu)(\gamma_2+\mu+d)\sigma_1}{\beta\sigma_2} + \frac{\omega\sigma_2\gamma_1\gamma_2}{(\gamma_1+\mu)(\gamma_2+\mu+d)} - \frac{(\alpha+\mu)\gamma_2}{\beta} + \frac{\omega\gamma_1[1-(\sigma_1+\sigma_2)]\gamma_3}{(\gamma_1+\mu)(\gamma_3+\mu+d)} - \frac{(\alpha+\mu)(\gamma_2+\mu+d)[1-(\sigma_1+\sigma_2)]\gamma_3}{\beta\sigma_2(\gamma_3+\mu+d)}\right] \quad (22)$$

V. Existence and Uniqueness of Solution

Initial conditions for the model equations (1)-(6) have a unique solution. In function form, model (1)-(5)'s initial equation looks like this:

$$\frac{dS}{dt} = f_1(\mathrm{S},\mathrm{t}) = \omega - \alpha\mathrm{S} - \mu\mathrm{S} - \beta S I_2$$

Both $f_1(\mathrm{S},\mathrm{t})$ and the partial derivative of $f_1(\mathrm{S},\mathrm{t})$ with regard to variable S are, of course, continuously defined. Also, keep in mind that,

$$|f_1(\mathrm{S}_1,\mathrm{t}) - f_1(\mathrm{S}_2,\mathrm{t})| = |\omega - \alpha\mathrm{S}_1 - \mu\mathrm{S}_1 - \beta\mathrm{S}_1 I_2 - \omega + \alpha\mathrm{S}_2 + \mu\mathrm{S}_2 + \beta\mathrm{S}_2 I_2|$$
$$|f_1(\mathrm{S}_1,\mathrm{t}) - f_1(\mathrm{S}_2,\mathrm{t})| = |-(\alpha+\mu)\mathrm{S}_1 + (\alpha+\mu)\mathrm{S}_2 - \beta I_2(\mathrm{S}_1 - \mathrm{S}_2)|$$
$$|f_1(\mathrm{S}_1,\mathrm{t}) - f_1(\mathrm{S}_2,\mathrm{t})| = |(\alpha+\mu)\mathrm{S}_2 - (\alpha+\mu)\mathrm{S}_1 - \beta I_2(\mathrm{S}_1 - \mathrm{S}_2)|$$
$$|f_1(\mathrm{S}_1,\mathrm{t}) - f_1(\mathrm{S}_2,\mathrm{t})| = |-(\alpha+\mu)(\mathrm{S}_1 - \mathrm{S}_2) - \beta I_2(\mathrm{S}_1 - \mathrm{S}_2)|$$
$$|f_1(\mathrm{S}_1,\mathrm{t}) - f_1(\mathrm{S}_2,\mathrm{t})| = |-(\alpha+\mu+\beta I_2)(\mathrm{S}_1 - \mathrm{S}_2)|$$
$$\leq m|\mathrm{S}_1 - \mathrm{S}_2|$$

Where $m = \alpha + \mu + \beta I_2 = \alpha + \mu + \frac{\omega\beta}{(\gamma_1+\mu)}\frac{\sigma_2\gamma_1}{(\gamma_2+\mu+d)} - (\alpha+\mu) = \frac{\omega\sigma_2\beta\gamma_1}{(\gamma_1+\mu)(\gamma_2+\mu+d)}$

Therefore, the Lipschitz condition holds.

The same is true for the other expressions; they can all be demonstrated. For all positive t, there exists a unique solution to the specified model, as proven by the Cauchy-Lipschitz theorem.

VI. Local Stability

Systems (1-5) have the following Jacobian matrices:

$$J = \begin{bmatrix} -(\alpha+\mu+\beta I_2) & 0 & -\beta S & 0 & 0 \\ \beta I_2 & -\gamma_1\mu & \beta S & 0 & 0 \\ 0 & \sigma_2\gamma_1 & -(\gamma_2+\mu+d) & 0 & 0 \\ 0 & [1-(\sigma_1+\sigma_2)]\gamma_1 & 0 & -(\gamma_3+\mu+d) & 0 \\ 0 & \sigma_1\gamma_1 & \gamma_2 & \gamma_3 & -\mu \end{bmatrix}$$

$$J = \begin{bmatrix} -a_1 & 0 & -a_2 & 0 & 0 \\ a_3 & -a_4 & a_5 & 0 & 0 \\ 0 & a_6 & -a_7 & 0 & 0 \\ 0 & a_8 & 0 & -a_9 & 0 \\ 0 & a_{10} & a_{11} & a_{12} & -a_{13} \end{bmatrix}$$

Where

$a_1 = \alpha + \mu + \beta I_2, a_2 = \beta S, a_3 = \beta I_2, a_4 = \gamma_1 \mu, a_5 = \beta S, a_6 = \sigma_2 \gamma_1, a_7 = \gamma_2 + \mu + d, a_8 = [1 - (\sigma_1 + \sigma_2)]\gamma_1, a_9 = \gamma_3 + \mu + d, a_{10} = \sigma_1 \gamma_1, a_{11} = \gamma_2, a_{12} = \gamma_3, a_{13} = \mu$

$k^5 + k^4((a_1 + a_4 + a_7 + a_9 + a_{13}) + k^3(a_1 a_9 + a_4 a_9 + a_4 a_{13} + a_5 + a_7 a_9 + a_7 a_{13} + a_9 a_{13} + a_8) + k^2((a_1 a_9 a_{13} + a_4 a_9 a_{13} + a_5 a_9 + a_{13} a_9 a_{13} + a_8 a_9 + a_8 a_{13}) + k(a_5 a_9 a_{13} + a_8 a_9 a_{13} + a_{11} a_{13}) + a_9 a_{11} a_{13} = 0$ (23)

For the reason that all the coefficients in the variables of Equation (23) are positive. So, if you follow the criteria of Routh and Hurwitz, you may rest assured that endemic equilibrium points are stable in their immediate vicinity.

VII. GLOBAL STABILITY

The following Lyapunov function is constructed to characterize the global stability at $(S^*, {I_1}^*, {I_2}^*, {I_3}^*)$.

We obtain by doing a differentiation of $W(S, I_1, I_2, I_3)$with regard to't'

$$W = \left[(S - S^*) - S^* log \frac{S}{S^*}\right] + m_1 \left[(I_1 - {I_1}^*) - {I_1}^* log \frac{I_1}{{I_1}^*}\right] + m_2 \left[(I_2 - {I_2}^*) - {I_2}^* log \frac{I_2}{{I_2}^*}\right] + m_3 \left[(I_3 - {I_3}^*) - {I_3}^* log \frac{I_3}{{I_3}^*}\right]$$

$$\frac{dW}{dt} = \left(\frac{S - S^*}{S}\right)\frac{dS}{dt} + m_1 \left(\frac{I_1 - {I_1}^*}{I_1}\right)\frac{dI_1}{dt} + m_2 \left(\frac{I_2 - {I_2}^*}{I_2}\right)\frac{dI_2}{dt} + m_3 \left(\frac{I_3 - {I_3}^*}{I_3}\right)\frac{dI_3}{dt}$$

$$\frac{dW}{dt} = \left(\frac{S - S^*}{S}\right)[\omega - \alpha S - \mu S - \beta S I_2] + m_1 \left(\frac{I_1 - {I_1}^*}{I_1}\right)[\beta S I_2 - \gamma_1 I_1 - \mu I_1] + m_2 \left(\frac{I_2 - {I_2}^*}{I_2}\right)(\sigma_2 \gamma_1 I_1 - \gamma_2 I_2 - \mu I_2 - d I_2) +$$

$$m_3 \left(\frac{I_3 - {I_3}^*}{I_3}\right)[\{1 - (\sigma_1 + \sigma_2)\}\gamma_1 I_1 - \gamma_3 I_3 - \mu I_3 - d I_3]$$

$$\frac{dW}{dt} = \left(\frac{S - S^*}{S}\right)[\omega - (\alpha + \mu + \beta I_2)S] + m_1 \left(\frac{I_1 - {I_1}^*}{I_1}\right)[\beta S I_2 - (\gamma_1 + \mu) I_1] + m_2 \left(\frac{I_2 - {I_2}^*}{I_2}\right)[(\sigma_2 \gamma_1 I_1 - (\gamma_2 + \mu + d) I_2] +$$

$$m_3 \left(\frac{I_3 - {I_3}^*}{I_3}\right)[\{1 - (\sigma_1 + \sigma_2)\}\gamma_1 I_1 - (\gamma_3 + \mu + d) I_3]$$

$$\frac{dW}{dt} = (S - S^*)\left[\frac{\omega}{S} - \frac{\omega}{S^*}\right] + m_1 (I_1 - {I_1}^*)\left[\beta S \frac{I_2}{I_1} - \beta S^* \frac{{I_2}^*}{{I_1}^*}\right] + m_2 (I_2 - {I_2}^*)\left[\left(\sigma_2 \gamma_1 \frac{I_1}{I_2} - \sigma_2 \gamma_1 \frac{{I_1}^*}{{I_2}^*}\right)\right] + m_3 \left(\frac{I_3 - {I_3}^*}{I_3} I_3 - {I_3}^*\right)\left[\{1 - (\sigma_1 + \sigma_2)\}\gamma_1 \frac{I_1}{I_3} - \{1 - (\sigma_1 + \sigma_2)\}\gamma_1 \frac{{I_1}^*}{{I_3}^*}\right]$$

$$\frac{dW}{dt} = (S - S^*)\left[\frac{\omega}{S} - \frac{\omega}{S^*}\right] + m_1 (I_1 - {I_1}^*)\left[\beta S \frac{I_2}{I_1} - \beta S^* \frac{{I_2}^*}{{I_1}^*}\right] + m_2 (I_2 - {I_2}^*)\left[\left(\sigma_2 \gamma_1 \frac{I_1}{I_2} - \sigma_2 \gamma_1 \frac{{I_1}^*}{{I_2}^*}\right)\right] + m_3 (I_3 - {I_3}^*)\left[\{1 - (\sigma_1 + \sigma_2)\}\gamma_1 \frac{I_1}{I_3} - \{1 - (\sigma_1 + \sigma_2)\}\gamma_1 \frac{{I_1}^*}{{I_3}^*}\right]$$

$$\frac{dW}{dt} = -\omega \frac{(S - S^*)^2}{S S^*} + \beta m_1 (I_1 - {I_1}^*)\frac{(S I_2 {I_1}^* - S^* I_1 {I_2}^*)}{I_1 {I_1}^*} + m_2 \sigma_2 \gamma_1 (I_2 - {I_2}^*)\frac{(I_1 {I_2}^* - {I_1}^* I_2)}{I_2 {I_2}^*} + m_3 \{1 - (\sigma_1 + \sigma_2)\}\gamma_1 (I_3 - {I_3}^*)\frac{(I_1 {I_3}^* - {I_1}^* I_3)}{I_3 {I_3}^*}$$

Let $m_1 = \frac{1}{\beta}, m_2 = \frac{1}{\sigma_2 \gamma_1}, m_3 = \frac{1}{\{1 - (\sigma_1 + \sigma_2)\}\gamma_1}$

$$\frac{dW}{dt} = -\omega \frac{(S - S^*)^2}{S S^*} + (I_1 - {I_1}^*)\frac{(S I_2 {I_1}^* - S^* I_1 {I_2}^*)}{I_1 {I_1}^*} + (I_2 - {I_2}^*)\frac{(I_1 {I_2}^* - {I_1}^* I_2)}{I_2 {I_2}^*} + (I_3 - {I_3}^*)\frac{(I_1 {I_3}^* - {I_1}^* I_3)}{I_3 {I_3}^*}$$

$$\frac{dW}{dt`} = -\omega \frac{(S - S^*)^2}{S S^*} + \frac{1}{I_1 {I_1}^*}\left[S I_2 I_1 {I_1}^* - S^* {I_1}^2 {I_2}^* - S I_2 {I_1}^{*2} + S^* I_1 {I_2}^* {I_1}^*\right] + \frac{1}{I_2 {I_2}^*}\left[I_1 {I_2}^* I_2 - {I_1}^* {I_2}^2 - I_1 {I_2}^{*2} + {I_1}^* I_2 {I_2}^*\right] + \frac{1}{I_3 {I_3}^*}\left[I_1 {I_3}^* I_3 - {I_1}^* {I_3}^2 - I_1 {I_3}^{*2} + {I_1}^* I_3 {I_3}^*\right]$$

$$\frac{dW}{dt} = -\omega \frac{(S - S^*)^2}{S S^*} + \left[S I_2 - S^* {I_2}^* \frac{I_1}{{I_1}^*} - S I_2 \frac{{I_1}^*}{I_1} + S^* {I_2}^*\right] + \left[I_1 - \frac{{I_1}^* I_2}{{I_2}^*} - \frac{I_1 {I_2}^*}{I_2} + {I_1}^*\right] + \left[I_1 - \frac{{I_1}^* I_3}{{I_3}^*} - \frac{I_1 {I_3}^*}{I_3} + {I_3}^*\right]$$

$$\frac{dW}{dt} = -\omega \frac{(S - S^*)^2}{S S^*} + \left[(S I_2 + S^* {I_2}^*) - \left(S^* {I_2}^* \frac{I_1}{{I_1}^*} + S I_2 \frac{{I_1}^*}{I_1}\right)\right] + \left[(I_1 + {I_1}^*) - \frac{{I_1}^* I_2}{{I_2}^*} - \frac{I_1 {I_2}^*}{I_2}\right] + \left[(I_1 + {I_3}^*) - \left(\frac{{I_1}^* I_3}{{I_3}^*} + \frac{I_1 {I_3}^*}{I_3}\right)\right]$$

Because of the fact that all RHS terms are negative: $\frac{dW}{dt} < 0$

The global asymptotic stability of the system (1)-(5) is proven via the Lyapunov theorem.

VIII. Basic Reproduction Number

The reproduction number is defined as the biggest Eigen value of the next-generation matrix V^{-1} .

$$\mathcal{F} = \begin{bmatrix} \beta S I_2 \\ 0 \\ 0 \end{bmatrix}, \mathcal{V} = \begin{bmatrix} \sigma_1\gamma_1 I_1 + \sigma_2\gamma_1 I_1 + (1-(\sigma_1+\sigma_2)\gamma_1 I_1 + \mu I_1 \\ -\sigma_2\gamma_1 I_1 + \gamma_2 I_2 + \mu I_2 + d I_2 \\ -(1-(\sigma_1+\sigma_2)\gamma_1 I_1 + +\mu I_3 + d I_3 \end{bmatrix}$$

$$F = \begin{bmatrix} \frac{\beta\omega}{\alpha+\mu} & 0 & 0 \\ 0 & 0 & 0 \\ 0 & 0 & 0 \end{bmatrix}, V = \begin{bmatrix} \gamma_1+\mu & 0 & 0 \\ -\sigma_2\gamma_1 & \gamma_2+\mu+d & 0 \\ \sigma_1+\sigma_2-1 & 0 & \mu+d \end{bmatrix}$$

$$V^{-1} = \begin{bmatrix} \frac{1}{\gamma_1+\mu} & 0 & 0 \\ \frac{\sigma_2\gamma_1}{(\gamma_1+\mu)(\gamma_2+\mu+d)} & \frac{1}{\gamma_2+\mu+d} & 0 \\ \frac{\sigma_1+\sigma_2-1}{(\gamma_1+\mu)(\mu+d)} & 0 & \frac{1}{\mu+d} \end{bmatrix}$$

$$FV^{-1} = \begin{bmatrix} \frac{\beta\omega}{\alpha+\mu} & 0 & 0 \\ 0 & 0 & 0 \\ 0 & 0 & 0 \end{bmatrix} \begin{bmatrix} \frac{1}{\gamma_1+\mu} & 0 & 0 \\ \frac{\sigma_2\gamma_1}{(\gamma_1+\mu)(\gamma_2+\mu+d)} & \frac{1}{\gamma_2+\mu+d} & 0 \\ \frac{\sigma_1+\sigma_2-1}{(\gamma_1+\mu)(\mu+d)} & 0 & \frac{1}{\mu+d} \end{bmatrix}$$

$$FV^{-1} = \begin{bmatrix} \frac{\beta\omega}{(\alpha+\mu)(\gamma_1+\mu)} & 0 & 0 \\ 0 & 0 & 0 \\ 0 & 0 & 0 \end{bmatrix}$$

$$R_0 = \frac{\beta\omega}{(\alpha+\mu)(\gamma_1+\mu)}$$

IX. Numerical Results and Discussion

Graph 1: Variation in all population associated to Time t

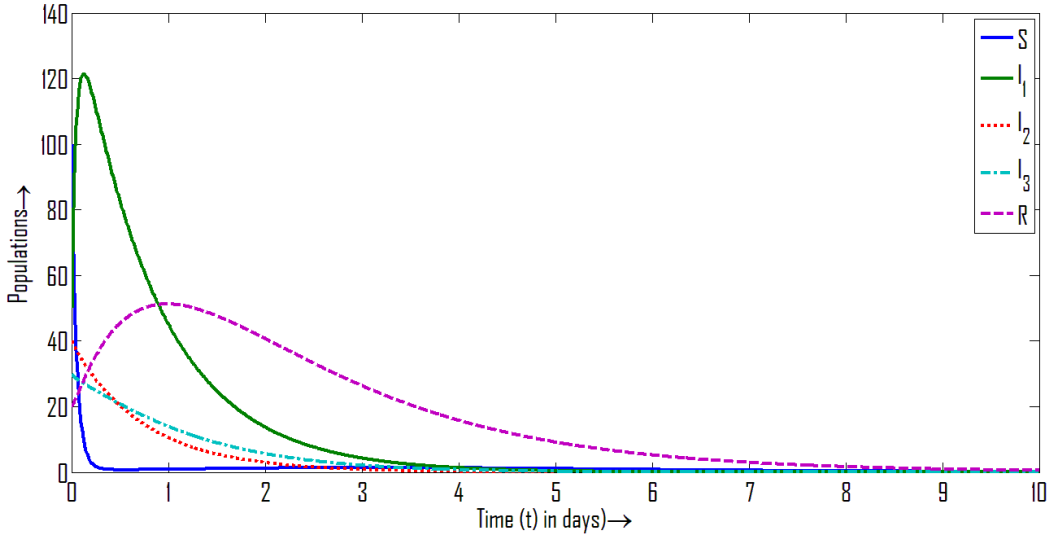

Graph 2:Mild Covid-19 infected population vs Time (day) for different infection rate

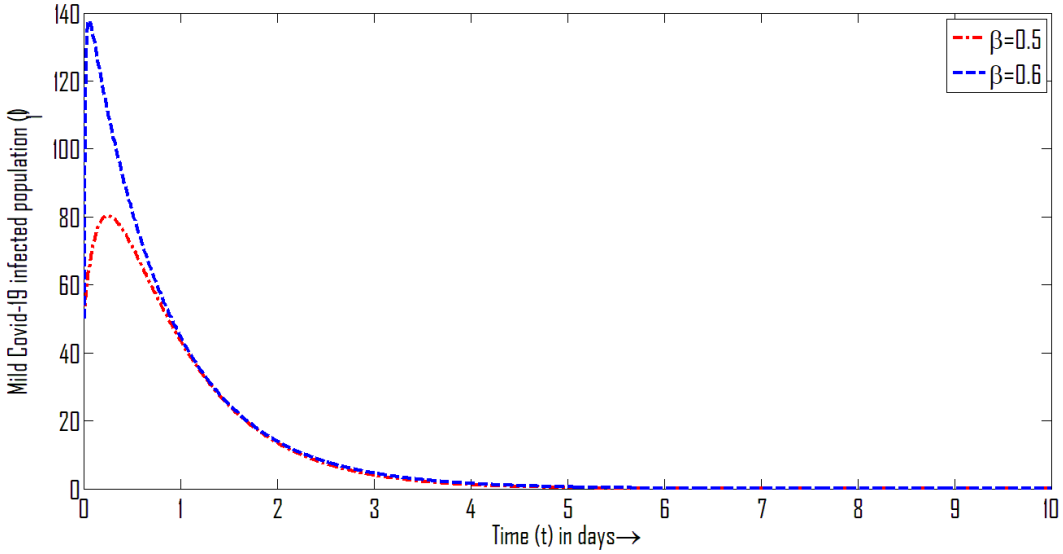

Graph 3:Recovered population vs time (day) for different recovery rate of mild infection

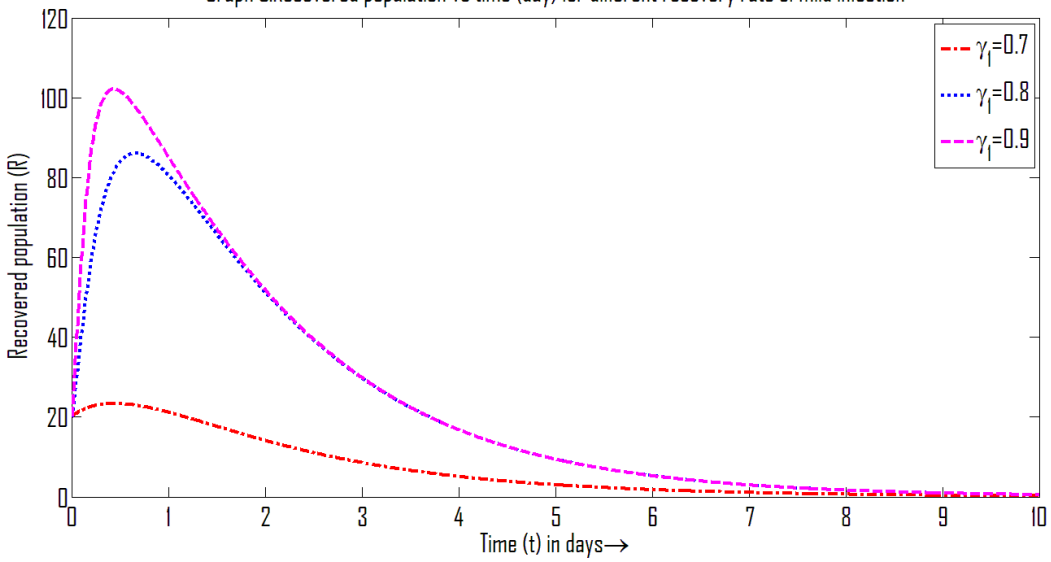

Graph 4:Recovered population vs Time (day) for different recovery rate of moderate infection

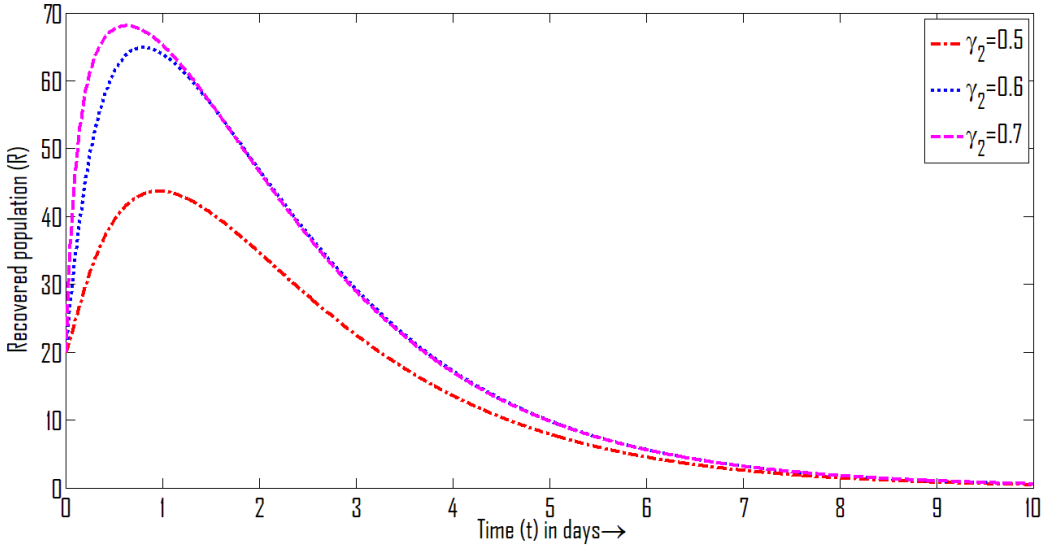

\

Graph 5: 3D plot of Recovered population for different infection rate of moderate Covid-19

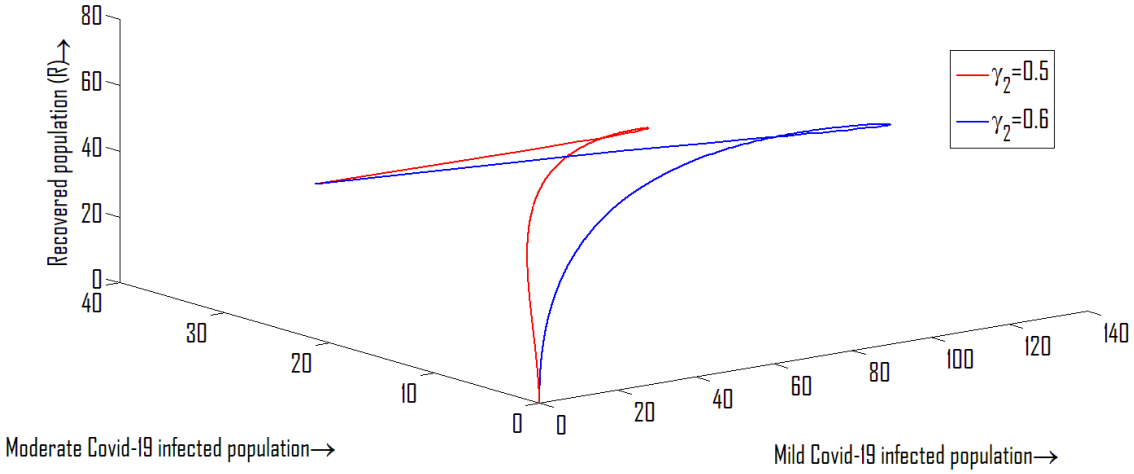

Graph 6:Severe Covid-19 infectious population vs Time (day) for different recovery rate of severe infection

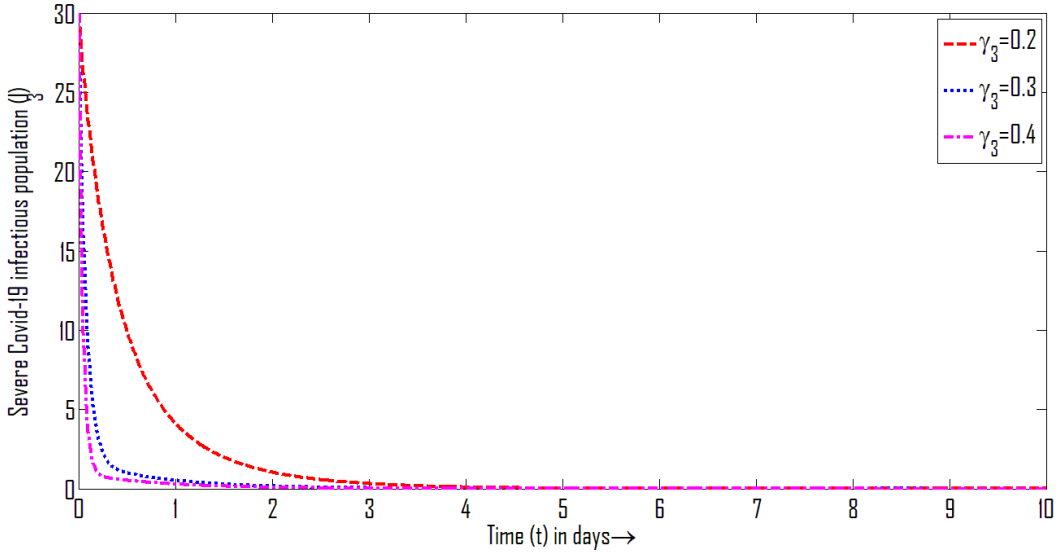

Graph 7:Recovered population (R) vs Time (day) for different recovery rate of severe infection

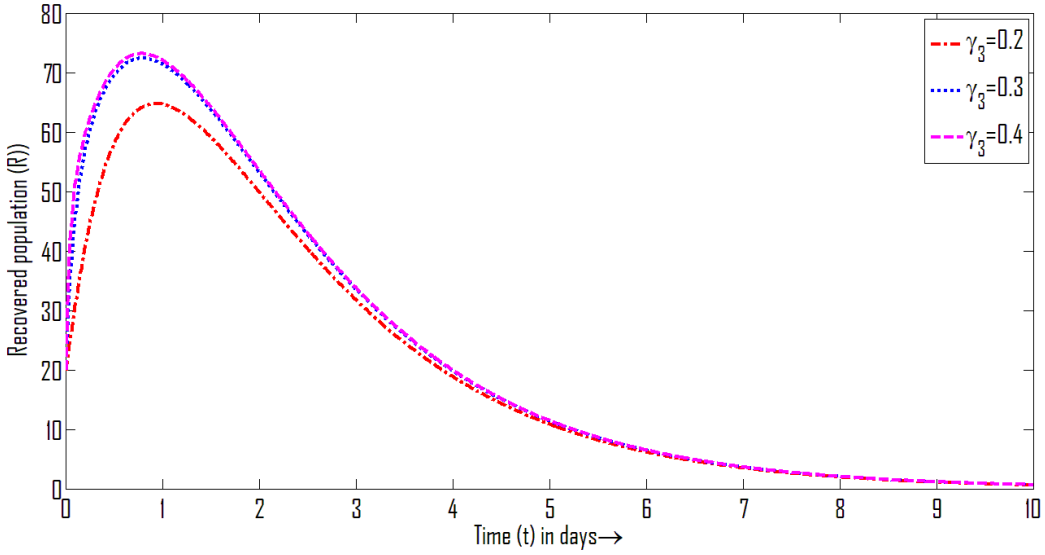

Graph 8:Mild Covid-19 infected population vs Time (day) for immunization rates

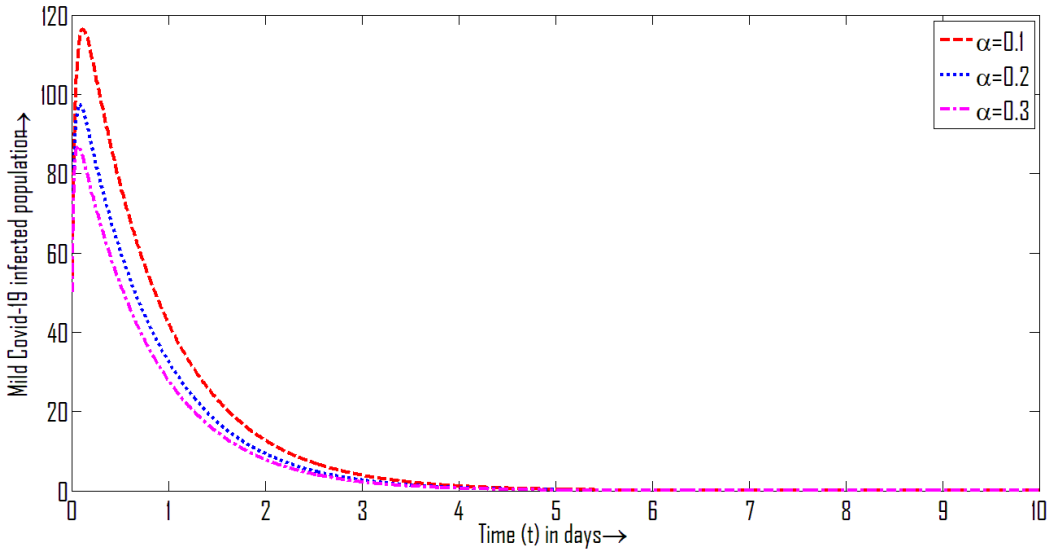

Graph 9: Recovered population (R) vs Time (day) for different immunization rates

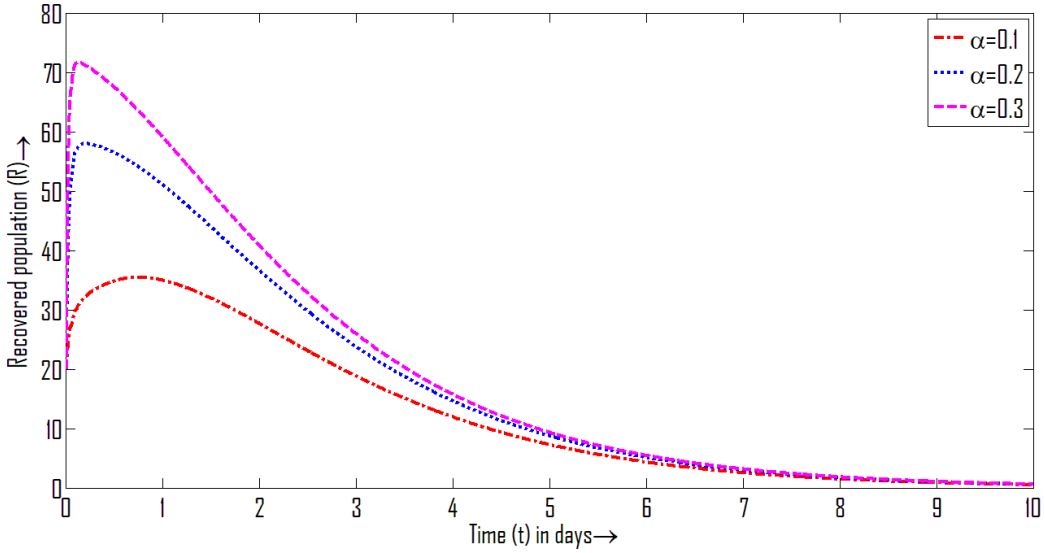

Graph 10: 3D plot of Recovered population for different different immunization rates

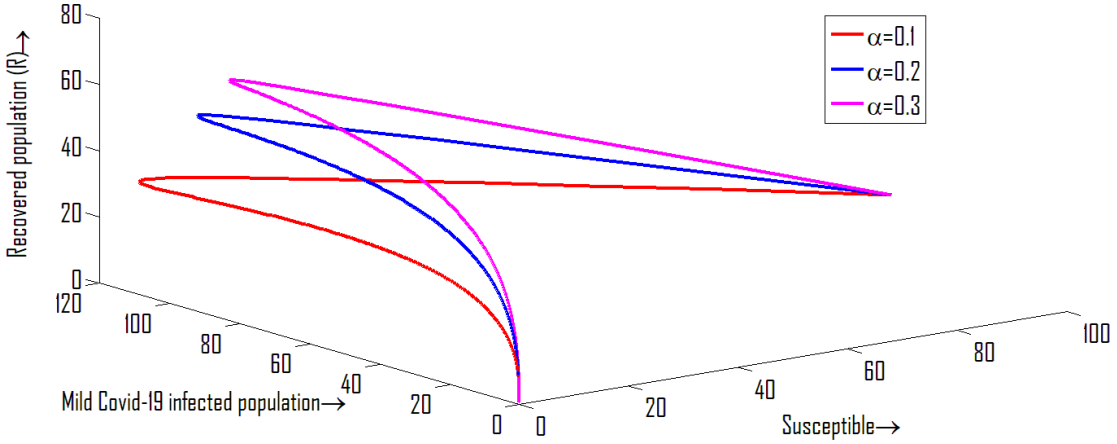

Graph (1) depicts the dynamics of our model, showing how the number of individuals in each group evolves over time. Graph (2) displays the change in the population of moderate Covid-19 infected individuals over time‘t’ for a range of values of the transition

infection rate. As the transition infectious rate rises, the number of people infected with moderate Covid-19 rises as well. Graph (3) displays how the recovered population shifts over time $'t'$ for varying values of the recovery rate from moderate infection by natural immunity. This chart shows that as the percentage of people who are able to recover from a mild infection rises, so does the population that has done so. Graph (4) displays the change in the recovered population over time $'t'$ for several values of the recovery rate from a moderate infection by natural immunity. This graph shows that as the percentage of people who have recovered from a moderate infection rises, so does the size of the recovered population. Graph (5) displays a three-dimensional (3D) comparison of the recovered population with the mild and moderate Covid-19 infected populations, illustrating the variation in recovery rates after moderate infection due to natural immunity. It is clear from this graph that the two trajectories meet at a single location. Graph (6) displays the time-dependent change in the proportion of the population infected with Covid-19 at the severe level, given varying values of the recovery rate from severe infection due to natural immunity. The population of people with severe cases of Covid-19 infection falls as the rate of recovery from severe illness rises, as seen in the graph below. If we look at graph (7), you can see how the recovered population shifts over time $'t'$ over a range of recovery rates after a severe infection due to natural immunity. This chart shows that as the percentage of people who make a full recovery from a serious infection rises, so does the size of the recovered population. Graph (8) displays the time-dependent change in the moderate Covid-19 infected population for a range of human recovery rates. This graph shows that as the rate of human recovery from mild Covid-19 infection raises, the population of people with the infection drops. The graph (9) below shows how the recovered population changes over time $'t'$ given a range of values for the recovery rate of susceptible persons. This graph shows that as the recovery rate of susceptible humans rises, so does the number of people who have been cured. Graph (10) displays a three-dimensional scatter plot of recovered populations including populations with mild Covid-19 infection and susceptible populations for varying rates of recovery of susceptible persons. It is clear from this graph that the three paths converge at the same place.

X. CONCLUDING REMARKS

Both the equilibrium locations and the basic reproduction number have been analytically demonstrated by mathematics in this work. We provide a model of Covid-19 where groups of humans experience mild, moderate, and severe infection with varying rates of recovery due to natural immunity. The model's solution and whether or not it exists and is unique, have also been explored. The model's local and global stability have been presented. Different population compartments' responses to the system parameters listed in table (1). Positive implications for preventing the spread of infectious illnesses can be drawn from policymakers' participation in ongoing efforts. Therefore, we wish for the government to increase the vigor of its regular initiatives to raise awareness and educate the people about the importance of taking precautions against the spread of contagious diseases.

REFERENCES

1. Akyildiz F.T., Alshammari F.S. (2021): “Complex mathematical SIR model for spreading of COVID-19 virus with Mittag-Leffler kernel”, Advances in Difference Equations, 319: 1-17.

2. Alanazi S.W., Kamruzzaman M.M., Alruwaili M., Alshammari N., Alqahtani S.A., Karime A. (2020): “Measuring and preventing covid-19 using the sir model and machine learning in smart health care, Journal of Healthcare Engineering”, Article ID 8857346, 12 pages.

3. Cooper I., Monda A., Antonopoulos C.G. (2020): “A SIR model assumption for the spread of COVID-19 in different communities”, Chaos, Solitons& Fractals, 139: 110057.

4. Franco C.M.R, Dutra R.F. (2021): “SIR model for propagation of COVID-19 in the Paraíba’s State (Brazil)”, Intermaths, 2(2):39-48.

5. Genga X.,.Katulb G.G. , Gergesa F., Bou-Zeide E., Nassiff H., Boufadela M.C. (2021): “A kernel-modulated SIR model for Covid-19 contagious spread from county to continent”, PNAS, 118(21):1-9.

6. Kotwal A., Yadav A.K, Yadav J., Kotwal J., Khune S. (2020): “Predictive models of COVID-19 in India: A rapid review”, Medical Journal Armed Forces India, 76:377-386.

7. Lakshmi V.N.S, Sabarmathi A. (2021): "A mathematical study on coronavirus model with two infectious states", Journal of Informatics and Mathematical Sciences, 13(2):71-81.

8. Malavika B. ,Marimuthu S. , Joy M. , Nadaraj A. , Asirvatham E.S , Jeyaseelan L. (2021): "Forecasting COVID-19 epidemic in India and high incidence states using SIR and logistic growth models", Clinically Epidemiology and Good health, 9:26-33.

9. Mallick P., Bhowmick S., Panja S. (2022): " Prediction of COVID-19 Infected Population for Indian States through a State Interaction Network-based SEIR Epidemic Model", IFAC Papers OnLine, 55(1):691-696.

10. Mohajan H.K. (2022): "Mathematical analysis of sir model for covid-19 transmission", Journal of Innovations in Medical Research, 1(2): 1-18.

11. Ram V. ,Schaposnik L.P. (2021): "A modified age structured SIR model for COVID-19 type viruses", Scientific Reports, 11:15194.

12. Saxena R., Jadeja M., Bhateja B. (2023): "Propagation analysis of covid-19: an sir model-based investigation of the pandemic", Arabian Journal for Science and Engineering, 48:11103-11115.